Medical and Research Publications
International Open Access

Research Article **Journal of MAR Case Reports (Volume 6 Issue 4)**

Assessment of Canalis Sinuous and it's Accessory Canals Via 3D Imaging Modality

Rasesh Shah *

Corresponding Author: Rasesh Shah, Department of Surgery, Hayatabad Medical Complex Peshawar.

Received Date: November 07, 2022

Published Date: December 01, 2022

Introduction

The anterior maxilla is subjected to a number of surgical procedures like removal of pathologies & foreign bodies, sinus floor elevation with staged or simultaneous placement of dental implants as well as orthognathic surgery (1). It has traditionally been regarded as a relatively safe site for surgery because the relatively fixed neurovascular structure in that area (2,3).

The neurovascular supply of this region is by the maxillary nerve and by the vessels accompanying this nerve. The infraorbital nerve provides sensory innervation to the skin and mid-face region. The anterior superior alveolar (ASA) nerve is a branch of infraorbital nerve and innervate incisors, canines, and associated soft tissues (4). Another important anatomical structure in the premaxilla is nasopalatine canal. The vessels and nerves passing through the canal supply the anterior teeth and soft tissues (5). There are many accessory foramina in this region and these anatomical variations of various size and morphological features can be misdiagnosed and mixed with apical pathologies (6).

An important but less frequently investigated anatomical structure which has a close anatomical relationship with the maxillary sinus is canalis sinuosus (CS). This canal contains anterior superior alveolar nerve (a branch of infraorbital nerve) and an accompanying artery and vein bundle. The CS is a tortuous bony channel that originates from the infraorbital canal posterior to the infraorbital foramen. From this point, the CS initially runs in an anterolateral direction towards the facial surface of the maxilla, then turns medially and inferiorly the infraorbital foramen, and progresses through the anterior wall of the maxillary antrum until it reaches the nasal aperture(7). It descends encircling the lateral and inferior edges of the pyriform aperture and finishes laterally on the anterior nasal spine, in a foramen called septal foramen.

The canalis sinuosus was first described and named by Jones in 1939. The name is based on its double curved course (7). It has several accessory canals as anatomic variations in the anterior maxilla(8), which are difficult to be recognized in 2D radiographs and rarely identified by clinicians(9,10). Panoramic and periapical radiographs used in routine are not sufficient to diagnose accessory channels due to some limitation (superimpositions, magnifications, distortions, low image quality). Thanks to the high resolution, cross sectional view and diagnostic reliability at lower costs and radiation doses advantages in dentistry, the use of CBCT has made it easier to diagnose these anatomical structures (11). Limited information about this anatomical structure and conventional radiography cannot reveal these accessory structures properly, it may make their diagnosis difficult, may lead to misdiagnosis, and may cause complications during or after surgical procedures (6,12).

Machado et al. and von Arx et al. identified a number of terminus locations of the CS and its accessory canals, with the majority terminating palatally, mesial to first premolars (13,14). In 2016, Machado et al (13) drew attention to the presence of the canal and presented 2 patients with postoperative pain because of canal injury during implant placement. Since then, patients with canal related neurovascular disturbances after an insertion of dental implants have been reported (4,15,16). The proximity of implant to the accessory canal is a hidden threat to postoperative complications including hemorrhage, paresthesia, and pain. Additionally, the presence of the accessory canal can affect the diffusion and penetration of local anesthetics, thus affecting the efficiency of anterior middle superior nerve block anesthesia (17). Characteristic information about such variants deserves more attention so as to provide anatomic guidance for implant surgeries. The proximity to the neurovascular bundle of CS and ACs can compromise osseointegration and cause temporary or permanent paresthesia as well as blood loss (2,15).

Previous studies focusing on additional canals perforating the anterior palatal cortex have reported a prevalence of anatomic variations ranging from 15.7% to 70.8% in the anterior maxilla (18–20). These canals may represent branches of the anterior superior alveolar nerve and also additional branches of nasopalatine nerve and nutrient canals (14,17). Ghandourah et al(12) reported a prevalence of 65.75% accessory canals of canalis sinuosus in 219 German participants. Tomrukcu et al(21) identified such canals in 34.7% of Turkish participants and reported that the region around the right lateral incisor was the predominant location.

Based on current literature, there are no studies performed on Indian population. Additionally, measurements performed by previous studies focused primarily on the prevalence and axial position of the accessory canal (22,23), without analyzing their potential relationship to the terminal canalis sinuosus and bone, which is essential to predict variations. Therefore, based on a large sample of cone beam computed tomography (CBCT) images, this retrospective study is aimed to analyze the diameter, and spatial position of accessory canals of the canalis sinuosus and explore their relationship to the characteristics of the terminal canalis sinuosus and anthropometric parameters in Indian population.

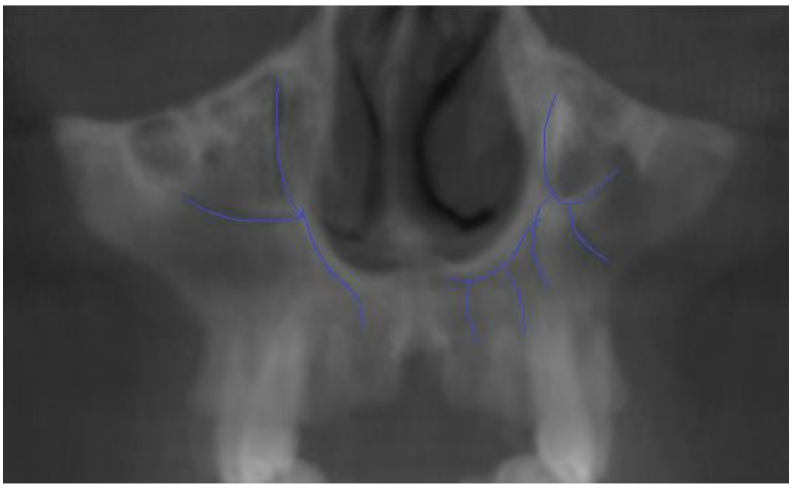

Figure 1: Variation in anatomy of right and left CS and ACS

Objective

Primary

To investigate and analyze the course of the canalis sinuosus (CS) until its termination in the anterior maxilla and chart its anatomical relationship with surrounding structures using CBCT.

Secondary

To identify the presence, frequency and characteristics of accessory canals (ACs) of CS in CBCT.

Rationale of the current study

Inadequate knowledge of the course of canalis sinuosus is often implicated in unexplained complications of anterior maxillary surgery such as paresthesia, hemorrhage & pain.

Study design: Retrospective study

Study setting: Patient cases are selected from the Department of Oral and maxillofacial surgery, Amrita School of Dentistry.

Selection process: The study population is composed of all patients who reported to the Department of Oral and Maxillofacial surgery for the management of mandibular pathology, maxillofacial trauma, dentofacial deformities, TMJ disorders and missing teeth.

Inclusion criteria

All patients who has normal maxillary anatomical landmarks in CBCT.

Exclusion criteria

1. Patients younger than 20 years old.
2. History of maxillary sinus trauma/surgery/orthognathic intervention.
3. The presence of a pathological lesion.
4. Supernumerary/impacted tooth or foreign bodies present.
5. Maxillary anterior tooth missing or alveolar bone loss that extended over 15% of root length
6. Artefact hindering image interpretation.

Material & Methods

All midface CBCT scans of maxillary anterior teeth, alveolar bone crest, and infra orbital rim; were collected from the Hospital. Images with radiographic noise that hindered measurements; presence of pathological lesions, midface trauma, presence of supernumerary or retained tooth in the anterior maxilla; history of surgical intervention in the anterior maxilla; with maxillary anterior tooth missing and alveolar bone loss that extended over 15% of root length were excluded.

A total of 180 CBCT scans were examined. All images were reconstructed by a software program (CS 3D Imaging Team). Measurements were performed in this software.

A standardized orientation with the hard palate parallel to the horizontal axis in the sagittal view was employed. Verifying and locating accessory canals in the 3D multiplanar reconstructions mode were carried out. This canal was identified in the sagittal and coronal plane, and its diameter was measured at the terminal level of canal opening in the axial plane. Only canals larger than 0.5-mm in diameter were included. The bifurcation site of the canalis sinuosus and terminal opening of the canal were marked. The distance from the inferior margin of the bifurcation site to the alveolar crest was measured to determine the sagittal position of the accessory canal.

Details of data to be collected

1. Presence or absence of ACs, frequency,
2. Rate of the identification of the CS using CBCT,
3. Distance b/w origin of the CS and the most inferior point of the orbital rim[Fig 2],
4. Distance b/w origin of the CS and anterior loop of the descending CS[Fig 3],
5. Distance b/w origin of the CS and floor of the nasal cavity[Fig 4],
6. Distance b/w origin of the CS and the infraorbital foramen[Fig 5],
7. Bifurcation site to buccal alveolar crest [Fig 6],
8. Diameter of the terminal canalis sinuosus, [Fig 8],
9. Distance from the terminal canalis sinuosus to the alveolar crest,
10. Distance b/w terminal canalis sinuosus and incisive canal[Fig 9].

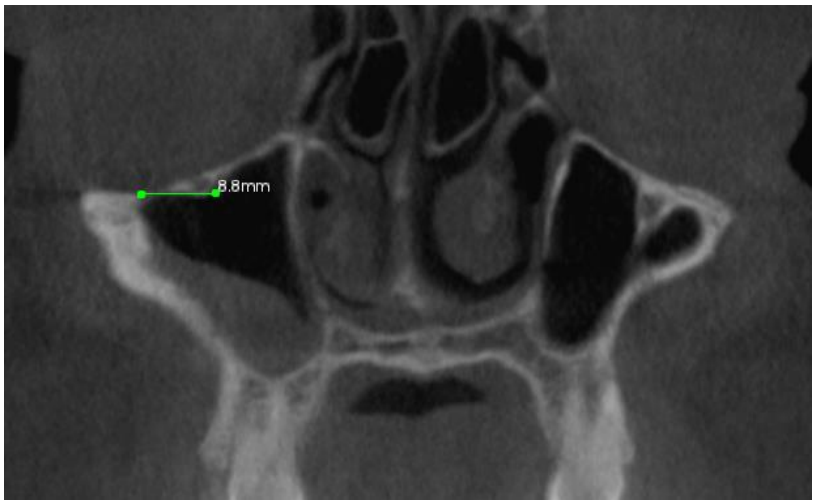

Figure 2: Distance b/w origin of CS and most inferior point of inferior orbital rim

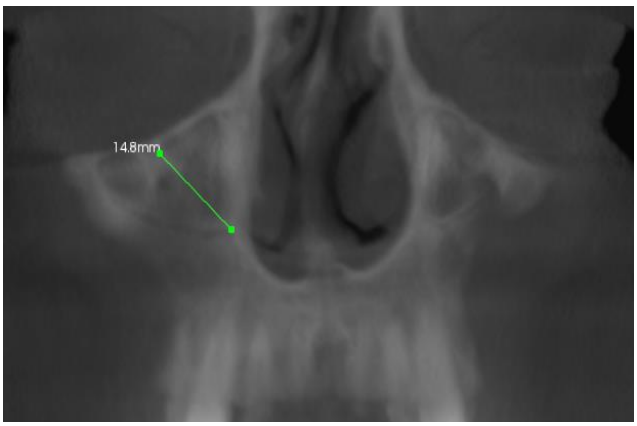

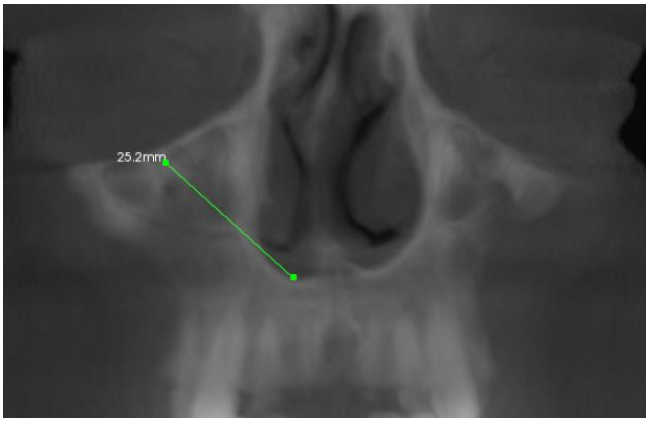

Fig 3: Distance b/w origin of CS and anterior loop of CS **Fig 4:** Distance b/w origin of CS and nasal floor

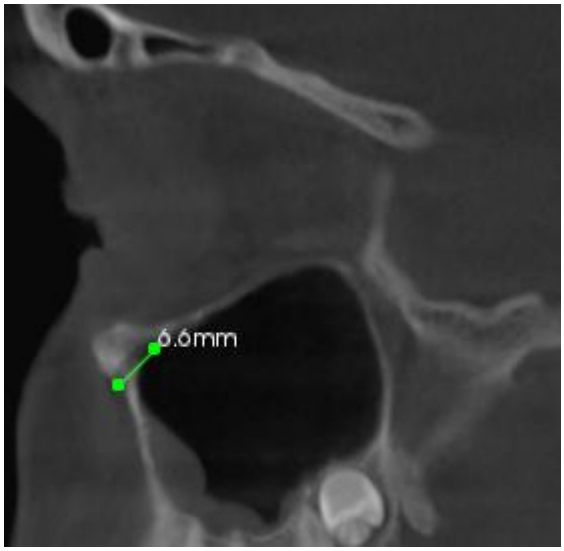

Fig 5: Distance b/w origin of CS and infra orbital foramen

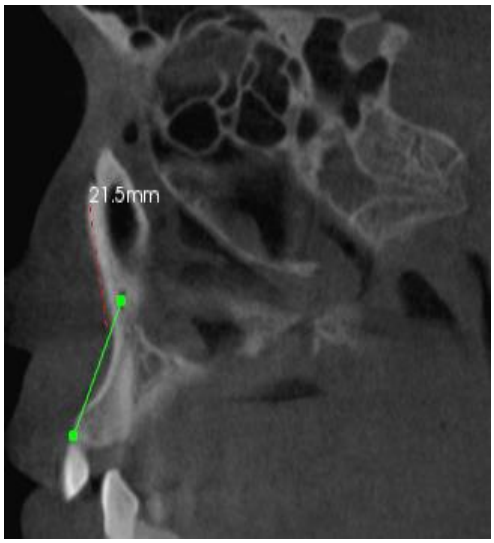

Fig 6: Distance b/w bifurcation of CS and buccal alveolar crest

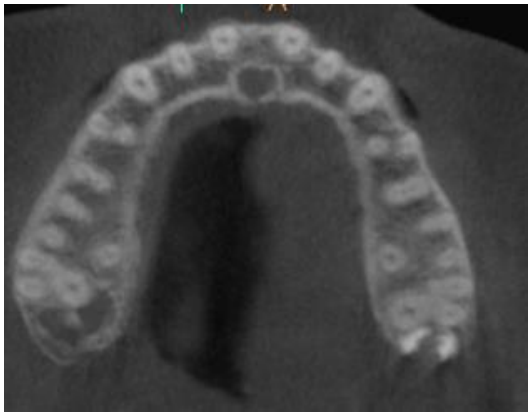

Fig 7: ACS terminal

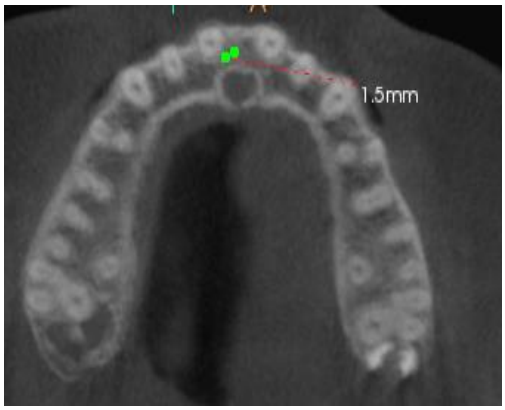

Fig 8: Diameter of ACS

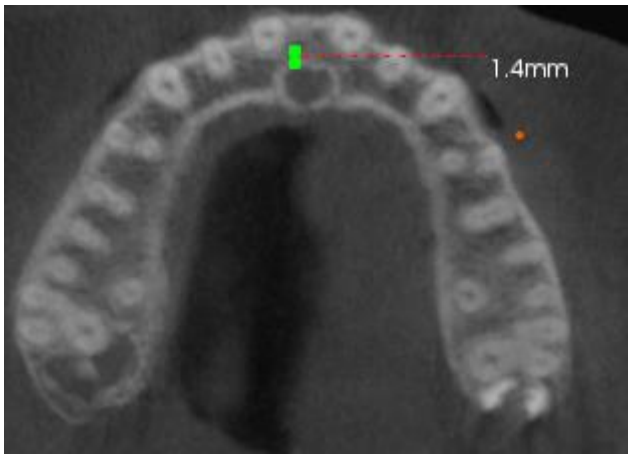

Fig 9: Distance b/w ACS and incisive canal

Results

Right Side

	Minimum(mm)	Maximum(mm)	Mean	Std. Deviation
Distance b/w origin of the CS and the most inferior point of the orbital rim	2.0	8.9	5.347	1.9890
Distance b/w origin of the CS and anterior loop of the descending CS	13.2	22.8	17.146	2.2238
Distance b/w origin of the CS and floor of the nasal cavity	23.7	34.5	29.286	2.7391
Distance b/w origin of the CS and the infraorbital foramen	4.5	14.0	7.249	2.0993
Bifurcation site to buccal alveolar crest	27.9	38.0	32.107	2.7106
Diameter of the terminal canalis sinuosus	.7	9.0	2.180	2.5811
Distance from the terminal canalis sinuosus to the buccal alveolar crest	1.9	5.5	3.927	1.0499
Distance from the canal opening to the palatal alveolar crest	1.5	9.9	6.443	2.4255
Distance b/w terminal canalis sinuosus and incisive canal	.9	9.1	5.030	2.4648

Table 1: Right side measurements

On right side, origin of CS is inferior to most inferior point of the orbital rim. Minimum and maximum distance is 2 and 8.9 mm respectively with mean of 5.3±1.98 mm. Minimum and maximum distance b/w origin of the CS and anterior loop of the descending CS is 13.2 and 22.8 mm respectively with a mean of 17.15±2.22. Minimum and maximum distance b/w origin of the CS and floor of the nasal cavity is 23.7 and 34.5 mm respectively with a mean of 29.29±2.74. Minimum and maximum distance b/w origin of the CS and the infraorbital foramen is 4.5 and 14 mm respectively with a mean of 7.23±2.1. Minimum and maximum distance from bifurcation site to buccal alveolar crest is 27.9 and 38 mm respectively with a mean of 32.11±2.71. Minimum and maximum diameter of the terminal

canalis sinuosus is 0.7 and 9 mm respectively with a mean of 2.18±2.58. Minimum and maximum distance from the terminal canalis sinuosus to the buccal alveolar crest is 1.9 and 5.5 mm respectively with a mean of 3.93±1.05. Minimum and maximum distance from the canal opening to the palatal alveolar crest is 1.5 and 9.9 mm respectively with a mean of 6.44±2.43. Minimum and maximum distance b/w terminal canalis sinuosus and incisive canal is 0.9 and 9.1 mm respectively with a mean of 5.03±2.46.

On left side, origin of CS is inferior to most inferior point of the orbital rim. Minimum and maximum distance is 2 and 4 mm respectively with mean of 3.02±0.37 mm. Minimum and maximum distance b/w origin of the CS and anterior loop of the descending CS is 16.2 and 21.3 mm respectively with a mean of 19.28±1.4. Minimum and maximum distance b/w origin of the CS and floor of the nasal cavity is 26 and 35 mm respectively with a mean of 29.04±1.66. Minimum and maximum distance b/w origin of the CS and the infraorbital foramen is 5.8 and 12.8 mm respectively with a mean of 9.1±1.98. Minimum and maximum distance from bifurcation site to buccal alveolar crest is 9.9 and 35.6 mm respectively with a mean of 24.69±7.63. Minimum and maximum diameter of the terminal canalis sinuosus is 0.7 and 8 mm respectively with a mean of 1.32±0.8. Minimum and maximum distance from the terminal canalis sinuosus to the buccal alveolar crest is 2.3 and 6.1 mm respectively with a mean of 4.44±1.09. Minimum and maximum distance from the canal opening to the palatal alveolar crest is 4 and 9 mm respectively with a mean of 6.58±1.42. Minimum and maximum distance b/w terminal canalis sinuosus and incisive canal is 2 and 6 mm respectively with a mean of 3.95±1.12.

Left Side

	Minimum(mm)	Maximum(mm)	Mean	Std. Deviation
Distance b/w origin of the CS and the most inferior point of the orbital rim	2	4	3.02	.365
Distance b/w origin of the CS and anterior loop of the descending CS	16.2	21.3	19.276	1.4005
Distance b/w origin of the CS and floor of the nasal cavity	26	35	29.04	1.657
Distance b/w origin of the CS and the infraorbital foramen	5.8	12.8	9.100	1.9787
Bifurcation site to buccal alveolar crest	9.9	35.6	24.687	7.6280

Diameter of the terminal canalis sinuosus	.7	8.0	1.316	.7987
Distance from the terminal canalis sinuosus to the buccal alveolar crest	2.3	6.1	4.439	1.0948
Distance from the canal opening to the palatal alveolar crest	4	9	6.58	1.420
Distance b/w terminal canalis sinuosus and incisive canal	2	6	3.95	1.115

Table 2: Left side measurements

Discussion

A number of studies investigating the course of CS used CT while others used CBCT. Olenczak et al. noted that CS was only identified in 15 (30%) of the 50 right hemiface CT scans and 14 (28%) in 50 left hemiface scans, despite using relatively thin 1 mm scan slices (24). This low rate of CS identification (29%) highlights the difficulty in using CT scans to investigate the CS anatomy when compared to the sensitivity of present day CBCT scans. A study by Wanzeler et al. reported 87.5% success in the identification of the CS using CBCTs using a basic voxel size of 0.250 mm, however, the FOV was not reported (25).

The prevalence of accessory canals of CS shows a wide range between 15.7% (19) and 70.8%(20), Oliviera Santos et al(19) which reported the lowest prevalence in the literature. Ghandourah et al (12) reported a prevalence as 67.6%. Significant difference between the prevalences may be derived from variety of reasons like methodological differences (voxel size, using of different CBCT scanners, different exposure parameters, inclusion/exclusion criterias etc), racial differences, study groups' distribution or may be just coincidental. The studies by Wanzeler et al. and Gurler et al. reported a frequency of CS as 88% and 100%, respectively (25,26). In comparison, the present study identified CS in 100% of cases using CBCT.

In a study by Temmermann et al. (18) limited to the canine area, it was reported that the canal always started at the palatal aspect of the canine to run in a latero-cranial direction. In the study by de Oliveira-Santos et al. (19), in 41.2 % a direct extension of accessory canals to the canalis sinuosus was described, but 52.9 % of canals were found to have an upward or oblique direction toward the anterior portion of the floor of the nasal cavity. The case presented by Neves et al. (9) is a well-documented

and correctly interpreted bilateral extension of the CS into the alveolar bone with exiting foramina palatal to the lateral incisors. In a case report by Kohavi(27), the author misinterpreted a wide bilateral tunnel along the pyriform aperture descending into the alveolar bone as a channel containing the posterior superior alveolar artery.

Machado et al. (13) reported a statistically significant difference of AC prevalence where they show male dominance, contrary to Machado, Sekerci et al(9) reported a girl's dominance in paediatric population(13). Von Arx et al (14), Oliviera Santos et al(19), Ghandourah et al(12), Orhan et al(20) show no significant difference between genders. In our study in the patients with ACs the male/female ratio was 0.88. This article is in agreement with previous studies in which gender differences were not statistically significant ($p = 0.544$).

Von Arx et al(14) reported increasing frequency of ACs with older ages and reported highest frequency in >60 year older group as 32,9%. But difference in age distribution and number of accessory canals per individual in different age groups were not significantly different.

Orhan et al reported highest frequency of AC in 50-59 age group(20). Machado reported the highest frequency at 41-60 age group as 55,1%. But they reported no significant difference between age groups (13). No statistically significant difference regarding the frequency of AC and the gender was reported by Oliveira Santos et al (19), Von Arx et al(14) and Orhan et al's studies(20). Machado et al(13) reported significantly higher prevalence in males (58%) than females (46,6%).

Oliveira-Santos et al. (19) showed a variation between the right and left sides regarding the distances between the CS and the alveolar bone crest and between the CS and the buccal cortical bone. This can be explained by the fact that the alveolar bone plate is subjected to morphological changes over time. In addition, this group revealed a greater number of patients ($n = 500$), which resulted in greater variations. They also highlighted that the foramen and canals in the anterior maxillary region are relatively frequent and that dental surgeons must be aware and well trained to identify these variations. In our study also, we found that same variation.

Von Arx et al. dissected 10 midface segments of five cadaver heads to chart the course of the anterior superior alveolar nerve present in CS(28). A study by Olenczak and co-workers included data from patients to investigate CS and post-traumatic midface pain(24). Fifty CT scans of the midface (50 patients bilaterally scanned) were examined to identify and measure the anatomical course of CS. The same study also included 12 adult cadavers resulting in an additional 24 data points. The cadaver dissection measurements of the distance between the anterior loop of the descending CS to the nasal

aperture returned a mean value of 3.4±0.5 mm, in comparison to the radiographically derived values from CT being 4.8±1.3 mm.

Table 3 Measurements (in mm) related to the CS course across comparative studies.

Measurements (mm)	Von Arx et al 2015[13](Cadaver)	Olenczak et al 2015[15](CT)	Hwang et al 2011[14](Cadaver)
Origin of the CS to the lateral margin of the IOF (BPh)	-2.8 ± 5.13	§	§
Superior margin of the IOF to the 90° bisecting line to the CS (CDv)	5.5 ± 3.07	§	§
Anterior loop of the descending CS to the nasal floor (EF'v)	13.6 ± 3.07	11.7 ± 3.0	§
Origin of the CS to the anterior loop of the descending CS (B'Eh)	§	12.9 ± 2.0	§
Anterior loop of the descending CS to the nasal aperture (EGh)	5.8 ± 1.96†	4.8 ± 1.3	0.8 ± 1.8†
	4.3 ± 2.74†	3.4 ± 0.5‡	2.6 ± 1.3†
	3.3 ± 2.60†		1.6 ± 0.9†

†Three measurements recorded at decreasing heights.
‡Cadaver measurement.
§Not reported.

The main result was that the ASAN is located, on average, 2.8 ± 5.13 mm lateral to the infraorbital foramen, running below the foramen at a mean distance of 5.5 ± 3.07 mm, making its correlation with the CS evident and emphasizing its importance in anesthesia of the anterior region of the maxilla(28). Olenczak et al. evaluated the course of ASAN through CS in human cadaver heads. They found a distance of 4.8 mm between the CS and the piriform aperture, pointing out that a better understanding of the course of the ASAN through this channel will guide future diagnosis for nerve injury and surgical intervention for patients with posttraumatic pain(24).

A study by Hwang et al. investigated the course of the superior alveolar artery while it progressed through the CS by dissecting 14 hemifaces of seven Korean adult cadavers(29). The study method involved three horizontal surgical cuts across the midface at specified levels to record the position of the CS. The course of the CS was recorded as it progressed from its anterior loop and descended alongside the nasal aperture. The highest vertical point measured between the nasal aperture and the descending CS was 0.8 ± 1.8 mm, the halfway point was 2.6 ± 1.3 mm and the lowest vertical measurement equaled 1.6 ± 0.9 mm. The measurements performed by Hwang et al. were shorter in comparison to the present study and the studies by von Arx et al. and Olenczak et al.(24,28,29). This discrepancy in results may be due to the fact that the study by Hwang and co-workers used a baseline through the most lateral border of the nasal aperture, which did not take the natural curvature of the aperture into account. Therefore, the measurements recorded related to the course of the CS were shorter. Taking an overview of the group of studies on this subject, each study used slightly differently defined measurement points for the horizontal measurements to ensure their respective reproducibility.

Machado et al(13) included the CS which they measured more than 1 mm in diameter such as Oliviera Santos et al(19), Von Arx et al(14) and Sekerci et al's study(30). In our study, the diameter of the CS evaluation was accepted to be at least 0,5 mm. The average diameter of the AC was 1.19 mm in Machado et al's study(13), which is similar to the average diameter of 1.31 mm reported by Von Arx et al(14), 1.2 mm by Sekerci et al(30), 1.4 mm in the analysis by Oliveira Santos et al(19). In our study, average distance between palatal ridge and opening of ACs is 6.4 mm and average of ACs median diameter is 1.32 mm. In average calculated foramens-canals, only canals-foramens wider than 0,5 mm included in the calculation. These values were close to the data obtained in previous studies.

In study by Wanzeler et al(25), the distance between CS's terminal portion and the region of alveolar ridge was observed as statistically significant differences associated to the gender. This distance was found to be higher in males than females. As Oliveira Santos et al(19) reported this difference in their studies, it was concluded that males may have differences of size, shape and bone density from females. Since alveolar ridge size is larger in males, it is natural that this distance is also vary from females. In a study by Manhaes Junior et al(8), they measured distance between the CS and buccal cortical bone and between CS and nasal floor. In the female group , there was a significant difference in favor of left side in distance between CS and buccal cortical bone measurement. When the results of male group were examined, it was seen that there were no differences between the sides for any of the measurements. In both group, there were no significant difference between the right and left sides in the distances from CS to nasal floor(8). In our study only significant relationship was seen between the gender (p=0,009) and palatal cortical bone distance. This distance was found to be higher in females than males. In both group, there were no significant difference between the right and left sides in the distances from CS to buccal cortical bone and nasal floor.

No statistically significant differences in the presence of the accessory canal was revealed regarding age or sex, consistent with the Brazilian results reported by Machado et al.(13) Although statistically higher frequency was reported in adults by Ghandourah et al(12) and in women by Aoki et al(22) their small sample size suggest that these results are unreliable. The accessory canal diameter was found to be 1.1 mm, smaller than the 1.19 mm and 1.30 mm in previous studies(13,21). Similar correlation between the diameter and the distance from the canal opening to the palatal alveolar crest indicated a tendency that canals with small calibers were more likely to open close to the alveolar crest. Given the small size of these canals, conventional radiography usually cannot adequately demonstrate their boundaries or locations. It is necessary to remind clinicians of the high prevalence of the canal in the anterior maxilla when interpreting conventional radiographs. The anterior maxilla, which has

traditional been regarded as a relatively safe site for implant placement(2,3), deserves more attention in surgical procedures.

Machado et al(13) suggested that the most common ends of the AC trajectories were located palatal to the anterior maxillary teeth (91.1%; 887/974), and less frequently in a buccal position (5.1%; 50/974) and in a transversal position (3.8%; 37/974). This study identified spatial locations of bifurcation sites and canal openings. Significant linear correlation between the distance from buccal alveolar crest to terminal canalis sinuosus and its bifurcation site indicated that the segment from where branches originated, coursed almost axially below the nasal floor. After running downward toward the alveolar ridge, all canals ended in the anterior palatal cortex. Their courses passing through the alveolar process make them susceptible to injury from procedures such as dental implant placement. The region between the central and the lateral incisors was a predominance location for the canal. Openings here and in the central incisor region were much closer to the alveolar crest than those between the lateral incisor and the canine. Combining frequency with opening position, the region around maxillary incisors appear to present more risks from accessory canals for implant placement. Clinicians must be vigilant about the orientation and depth of the implant placed in the alveolar bone to avoid neurovascular injury. The distance between canal opening and alveolar crest may act as an individual indicator in maxillary surgery to determine the safe zone for implant placement and bone harvesting.

Wanzeler et al.(25) noted the location of terminal segment of CS and; made measurements of diameter of canal at two points: where it branches from infraorbital canal, and where it ends. In their work, 12.58 % of evaluated canals extend to the palate, corresponding to anatomic variations according to the criteria of this study. Furthermore, aberrant location of terminal portion of the canal that is, at the apex of the teeth or near the apex, in the maxillary sinus, or the alveolar ridges- was observed in 40.58 % of images. We observed in our study that majority of canal opens near palatal ridge and apex of the incisors..

Furthermore, Von Arx et al.(14) found aberrant extensions of CS more frequently in left side. In contrast, de Oliveira-Santos et al.(19) observed bilateral accessory foramen in palate, similar to what is reported in present study, in which anatomic variations for CS appear predominantly bilaterally.

Vâlcu et al.(31) reported anatomic variation of CS in the hard palate that was interpreted as a possible aberrant fissure of the maxilla, but may have been an anatomic variation of the CS.

Table IV. Analysis of data in publications about canalis sinuosus.

Author	Year	Population	Sample size	Type of simple	Study objective
de Oliveira-Santos *et al.*	2013	Brazil	178	CBCT	Presence of foramina and accessory canals in the anterior region of the palate, some of which (7.86 %) correspond to extensions of CS.
Von Arx *et al.*	2013	Switzerland	176	CBCT	Presence of accessory canals in the anterior region of the maxilla, some of which (56.7 %) correspond to extensions of CS.
Manhães *et al.*	2016	Brazil	500	CBCT	Presence of CS (36.2 %), laterality and distance to adjacent anatomic structures (terminal segment).
Machado *et al.*	2016	Brazil	1000	CBCT	Prevalence of accessory canals of CS, distance to adjacent structures and relationship to demographic variables.
Gurler *et al.*	2017	Turkey	111	CBCT	Study of the pathway of CS. Morphometric measurements from CS to adjacent impacted canines.
Baena *et al.* (Current study)	2019	Colombia	236	CBCT	Prevalence of CS (100 %), frequency of its anatomic variations (46 %), variations by segments of CS and relationship to demographic variables.

The clinician's knowledge about the anatomical variations decrease complication possibility and increase the prognosis(4). Neurovascular bundles in anterior maxilla are important. Due to surgical procedures, they may damage the structures and cause sensory dysfunction (hyperesthesia, paraesthesia or pain) and haemorrhage. Also these bundles may alter the osseointegration and may lead to failure of implants. Lastly, they may mimic a lesion and can cause diagnostic confusion. Shah et al reported a case in which accessory branch of CS was mistakenly diagnosed as an external root resorption at periapical radiographies(6,13,19).

The location and course of CS and its neurovascular structures make it susceptible to injury following surgical interventions or trauma to the region. Indeed, other surgical procedures such as Le Fort 1 osteotomies and canine fossa puncture or antrostomy carry a much higher risk of trauma to the CS(32–34). During this procedure, the canal is cut, thus causing a direct injury to the anterior superior alveolar neurovascular bundle with possible complications such as bleeding and dysesthesia (Vâlcu et al.; de Oliveira-Santos et al.)(19). Placement of dental implants in the anterior region of the maxilla without prior assessment of the position and the characteristics of the canal may lead to iatrogenic injury because placement of an implant inside the canal may be associated with pain and difficulty during osseointegration(9,19,35). Some studies have explored new techniques to try and reduce this risk, for example a study by Tan et al. used transillumination of the maxillary sinus to help identify and avoid CS during canine fossa puncture(36). The placement of dental implants is a common undertaking by general dentists, who may not have undergone extensive oral surgery training and/or be less knowledgeable regarding the anatomical intricacies of the maxilla. Over the last 15 years, a number of

studies have detailed neurological or bleeding complications following implant placement where CS is impinged upon(4,10,15,37–41). It is unclear as to why symptoms vary when there is potential impingement on CS following dental implant placement. For instance the percentage of patients who presented with at least one accessory canal from the CS in the anterior maxilla ranges from 28% to 51%(13,14), however, this is not reflected in the low number of reported adverse sequelae in the literature. Most studies, however, do not detail whether it is the main CS canal or an accessory branch which has been impinged upon. Machado et al report a case who had pain after implant insertion with a close relation to accessory canal and immediate relief after removal of the implant(13).

Surgeons planning interventions in regions containing the CS need to be aware of its presence and there may be a benefit in being able to identify it as part of their pre-surgical workup, to minimize the risk of iatrogenic harm to the patient.

Conclusion

CS is an anatomical structure between the alveolar ridges on the lateral wall of the nasal cavity. The CS may present variations with regard to its location, diameter, and course, but there were no statistically significant differences with regard to age or gender. The CS involves the ASAN, manifesting extensions to the ACs in the anterior palate region. It is known that complications such as nerve damage, haemorrhage, unexpected bleeding as a result of damage of ASA nerves and its branches. So it is important that in surgical procedures of anterior maxillary region, identification of CS and its accessory branches helps in avoiding injuries.

The present radiographic study has evaluated the course of CS related to local anatomical landmarks and has revealed minor variations may occur in path of this bony channel. The rate of identification of the CS using CBCT was 100%. This suggests that CBCT would be the investigative method of choice for identification of CS. Statistically significant differences were seen in the course of CS between the left and right-sided scans. It is suggested that clinicians planning interventions in the region of CS could benefit from this data, which may help to reduce the occurrence of iatrogenic neurovascular complications.

References

1. Bornstein MM, Balsiger R, Sendi P, von Arx T. Morphology of the nasopalatine canal and dental implant surgery: a radiographic analysis of 100 consecutive patients using limited cone-beam computed tomography. Clin Oral Implant Res 2011;22:295–301.

2. Jacobs R, Quirynen M, Bornstein MM. Neurovascular disturbances after implant surgery. Periodontol 2000 2014;66:188-202.

3. Taschieri S, Weinstein T, Rosano G, Del Fabbro M. Morphological features of the maxillary incisors roots and relationship with neighbouring anatomical structures: possible implications in endodontic surgery. Int J Oral Maxillofac Surg 2012;41:616-23.

4. Arruda JA, Silva P, Silva L, Álvares P, Silva L, Zavanelli R, et al. Dental implant in the canalis sinuosus: a case report and review of the literature. Case Rep Dent 2017;2017:1-5.

5. Mraiwa N, Jacobs R, Van Cleynenbreugel J, Sanderink G, Schutyser F, Suetens P, van Steenberghe D, Quirynen M. The nasopalatine canal revisited using 2D and 3D CT imaging. Dentomaxillofac Radiol. 2004;33:396-402.

6. Shah PN, Arora AV, Kapoor SV. Accessory branch of canalis sinuosus mimicking external root resorption: A diagnostic dilemma. J Conserv Dent. 2017;20:479-81.

7. Jones FW. The anterior superior alveolar nerve and vessels. J Anat 1939;73: 583-91.

8. Manhaes Junior LR, Villaca-Carvalho MF, Moraes ME, Lopes SL, Silva MB, Junqueira JL. Location and classification of canalis sinuosus for cone beam computed tomography: avoiding misdiagnosis. Braz Oral Res 2016;30:e49.

9. Neves FS, Crusoé-Souza M, Franco LCS, Caria PHF, Bonfim-Almeida P, Crusoé-Rebello I. Canalis sinuosus: a rare anatomical variation. Surg Radiol Anat 2011;34:563-6.

10. Shelley A, Tinning J, Yates J, Horner K. Potential neurovascular damage as a result of dental implant placement in the anterior maxilla. Br Dent J 2019;226: 657-61.

11. Allareddy V, Vincent SD, Hellstein JW, Qian F, Smoker WR, Ruprecht A. Incidental findings on cone beam computed tomography images. Int J Dent. 2012;2012:871532.

12. Ghandourah AO, Rashad A, Heiland M, Hamzi BM, Friedrich RE. Conebeam tomographic analysis of canalis sinuosus accessory intraosseous canals in the maxilla. Ger Med Sci 2017;15.

13. Machado VC, Chrcanovic BR, Felippe MB, Manhaes Junior LR, de Carvalho PS. Assessment of accessory canals of the canalis sinuosus: a study of 1000 cone beam computed tomography examinations. Int J Oral Maxillofac Surg 2016;45:1586-91.

14. von Arx T, Lozanoff S, Sendi P, Bornstein MM. Assessment of bone channels other than the nasopalatine canal in the anterior maxilla using limited cone beam computed tomography. Surg Radiol Anat 2013;35:783-90.

15. McCrea SJJ. Aberrations causing neurovascular damage in the anterior maxilla during dental implant placement. Case Rep Dent 2017;2017:5969643.

16. Volberg R, Mordanov O. Canalis sinuosus damage after immediate dental implant placement in the esthetic zone. Case Rep Dent 2019;2019: 3462794.

17. Cetkovic D, Antic S, Antonijevic D, Brkovic BMB, Djukic K, Vujaskovic G, et al. Nutrient canals and porosity of the bony palate: a basis for the biological plausibility of the anterior middle superior alveolar nerve block. J Am Dent Assoc 2018;149:859-68.

18. Temmerman A, Hertele S, Teughels W, Dekeyser C, Jacobs R, Quirynen M. Are panoramic images reliable in planning sinus augmentation procedures? Clin Oral Implants Res 2011;22:189-94.

19. de Oliveira-Santos C, Rubira-Bullen IR, Monteiro SA, Leon JE, Jacobs R. Neurovascular anatomical variations in the anterior palate observed on CBCT images. Clin Oral Implants Res 2013;24:1044-8.

20. Orhan K, Gorurgoz C, Akyol M, Ozarslanturk S, Avsever H. An anatomical variant: evaluation of accessory canals of the canalis sinuosus using cone beam computed tomography. Folia Morphol (Warsz) 2018;77:551-7.

21. Tomrukcu DN, Kose TE. Assesment of accessory branches of canalis sinuosus on CBCT images. Med Oral Patol Oral Cir Bucal 2020;25:e124-30.

22. Aoki R, Massuda M, Zenni LTV, Fernandes KS. Canalis sinuosus: anatomical variation or structure? Surg Radiol Anat 2019;42:69-74.

23. Anatoly A, Sedov Y, Gvozdikova E, Mordanov O, Kruchinina L, Avanesov K, et al. Radiological and morphometric features of canalis sinuosus in russian population: cone-beam computed tomography study. Int J Dent 2019;2019:2453469.

24. Olenczak JB, Hui-Chou HG, Aguila DJ 3rd, Shaeffer CA, Dellon AL, Manson PN. Posttraumatic midface pain: clinical significance of the anterior superior alveolar nerve and canalis sinuosus. Ann Plast Surg 2015;75:543–7.

25. Wanzeler AMV, Marinho CG, Junior SMA, Manzi FR, Tuji FM. Anatomical study of the canalis sinuosus in 100 cone beam computed tomography examinations. Oral Maxillofac Surg. 2015;19:49–53.

26. Gurler G, Delilbasi C, Ogut EE, Aydin K, Sakul U. Evaluation of the morphology of the canalis sinuosus using cone-beam computed tomography in patients with maxillary impacted canines. Imaging Sci Dent. 2017;47:69-74.

27. Kohavi D (1994) Demonstration of unusually wide artery in the maxillary alveolar bone using a reformatting program of computed tomography: a case report. Int J Oral Maxillofac Implants 9:444–448.

28. von Arx T, Lozanoff S. Anterior superior alveolar nerve (ASAN). Swiss Dent J 2015;125:1202–9.

29. Hwang K, Kim DH, Kim DJ. Anterior superior alveolar artery and horizontal maxillary osteotomy. J Craniofac Surg 2011;22:1819–21.

30. Sekerci AE, Cantekin K, Aydinbelge M. Cone beam computed tomographic analysis of neurovascular anatomical variations other than the nasopalatine canal in the anterior maxilla in a pediatric population. Surg Radiol Anat. 2015;37:181-6.

31. Vâlcu, M.; Rusu, M. C.; Sendroiu, V. M. & Didilescu, A. C. The lateral incisive canals of the adult hard palate - aberrant anatomy of a minor form of clefting? Rom. J. Morphol. Embryol., 52(3):947-9, 2011.

32. Rosenberg A, Sailer HF. A prospective study on changes in the sensibility of the oral mucosa and the mucosa of the upper lip after Le Fort I osteotomy. J Cranio-maxillo-fac Surg 1994;22:286–93.

33. Thygesen TH, Bardow A, Norholt SE, Jensen J, Svensson P. Surgical risk factors and maxillary nerve function after Le Fort I osteotomy. J Oral Maxillofac Surg 2009;67:528–36.

34. Robinson S, Wormald PJ. Patterns of innervation of the anterior maxilla: a cadaver study with relevance to canine fossa puncture of the maxillary sinus. Laryngoscope 2005;115:1785–8.

35. Al-Khabbaz, A. K.; Griffin, T. J. & Al-Shammari, K. F. Assessment of pain associated with the surgical placement of dental implants. J. Periodontol., 78(2):239-46, 2007.

36. Tan NC, Floreani SR, Robinson S, Nair S, Sunkaraneni VS, Faris C et al. Transillumination-assisted maxillary trephination: cadaver validation of a new technique. Laryngoscope. 2009;119:984–7.

37. Kalpidis CD, Setayesh RM. Hemorrhaging associated with endosseous implant placement in the anterior mandible: a review of the literature. J Periodontol. 2004;75:631–45.

38. Hong YH, Mun SK. A case of massive maxillary sinus bleeding after dental implant. Int J Oral Maxillofac Surg 2011;40:758–60.

39. Rodriguez-Lozano FJ, Sanchez-Perez A, Moya-Villaescusa MJ, Rodriguez-Lozano A, Saez-Yuguero MR. Neuropathic orofacial pain after dental implant placement: review of the literature and case report. Oral Surg Oral Med Oral Pathol Oral Radiol Endod 2010;109:e8–12.

40. Devine M, Taylor S, Renton T. Chronic post-surgical pain following the placement of dental implants in the maxilla: a case series. Eur J Oral Implantol 2016;9(Suppl. 1):179–86.

41. Politis C, Agbaje J, Van Hevele J, Nicolielo L, De Laat A, Lambrichts I et al. Report of neuropathic pain after dental implant placement: a case series. Int J Oral Maxillofac Implants 2017;32: 439–44.